Journal of Loss Prevention in the Process Industries 26 (2013) 1501–1505

Contents lists available at ScienceDirect

Journal of Loss Prevention in the Process Industries

journal homepage: www.elsevier.com/locate/jlp

Flame acceleration in unconfined hydrogen/air deflagrations using infrared photography

Woo Kyung Kim [a,*], Toshio Mogi [b], Ritsu Dobashi [a]

[a] Department of Chemical System Engineering, The University of Tokyo, Japan
[b] Graduate School of Engineering, The University of Tokyo, Japan

ARTICLE INFO

Article history:
Received 22 December 2012
Received in revised form
26 September 2013
Accepted 28 September 2013

Keywords:
Flame acceleration
Self-acceleration
Flame front instability
Blast wave
Gas explosion
Hydrogen

ABSTRACT

Flame behavior and blast waves generated during unconfined hydrogen deflagrations were experimentally studied using infrared photography. Infrared photography enables expanding spherical flame behaviors to be measured and flame acceleration exponents to be evaluated. In the present experiments, hydrogen/air mixtures of various concentrations were filled in a plastic tent of thin vinyl sheet of 1 m^3 and ignited by an electric spark. The onset of accelerative dynamics on the flame propagation was analyzed by the time histories of the flame radius and the stretched flame speed. The results demonstrated that the self-acceleration of the flame, which was caused by diffusional-thermal and hydrodynamic instabilities of the blast wave, was influenced by hydrogen deflagrations in unconfined areas. In particular, it was demonstrated that the overpressure rapidly increased with time. The burning velocity acceleration was greatly enhanced with spontaneous-turbulization.

1. Introduction

To maintain safety standards against accidental hydrogen explosions, the behaviors of confined and unconfined hydrogen explosions were investigated (Dorofeev, 2007; Groethe et al., 2007; Lobato, Cañizares, Rodrigo, Sáez, & Linares, 2006; Molkov, Makarov, & Schneider, 2006; Otsuka, Saitoh, Mizutani, Morimoto, & Yoshikawa, 2007; Wakabayashi et al., 2007). During a hydrogen explosion, an increase in pressure due to flame propagation is an important parameter that needs to be considered to determine proper safety management. The pressure variation depends strongly on the flame acceleration in both confined and unconfined hydrogen explosions (Dobashi, Kawamura, Kuwana, & Nakayama, 2011; Nishimura, Mogi, & Dobashi, 2013). In unconfined gas explosions, the pressure wave is dramatically increased by flame acceleration. The results show that the maximum overpressure was higher than that evaluated by an acoustic model at a constant velocity (Dobashi et al.., 2011; Kim, Mogi, & Dobashi, 2013). The maximum overpressure during unconfined gas explosions was strongly affected by the accelerative motions of flame propagation from the excitation mechanisms of the flame front, which include hydrodynamic and diffusional-thermal instabilities. The acceleration due to the flame front instabilities may have caused the considerable damage during large-scale hydrogen deflagrations.

Many studies have been performed to understand the accelerative phenomena of the hydrogen flame (Bradley, 1999; Bradley, Cresswell, & Puttock, 2001; Bradley & Harper, 1994; Bradley, Hicks, Lawes, Sheppard, & Woolley, 1998; Dorofeev, 2007; Gostintsev, Fortov, & Shatskikh, 2004; Gostintsev, Istratov, & Shulenin, 1988; Molkov et al.., 2006). From experimental data, Gostintsev et al. (2004, 1988) suggested a power-law expression of similar turbulent flame propagations associated with fractal theory:

$$r = r^* + A(t - t^*)^{1.5} \quad (1)$$

where A is constant associated with the mixtures and r^* and t^* are the critical flame radius and the onset time of self-turbulization, respectively. It was reported the critical flame radius and time for the onset of a self-similar turbulization of stoichiometric hydrogen/air mixture were $r^* = 1.0–1.2$ m, $t^* = 0.04$ s in Gostintsev et al. (1988).

Bradley et al. (2001) analyzed the onset of flame cracking instabilities at a critical Peclet number, Pe_{cr}. The flame was modeled as a fully cellular structure and correlated with increases in flame speed, at the critical cellular Peclet number, Pe_{cl}. When analyzing

* Corresponding author.
E-mail addresses: youwoo2@gmail.com, youwoo2@hotmail.com (W.K. Kim).

0950-4230/$ – see front matter © 2013 Elsevier Ltd. All rights reserved.
http://dx.doi.org/10.1016/j.jlp.2013.09.009

the experimental data from methane and propane in air in large-scale explosions, they suggested that the transition from the flame to self-turbulization occurred at a considerably lower critical number than predicted (Gostintsev et al., 1988). Because the onset of flame acceleration is important in evaluating large-scale unconfined hydrogen explosions, the accelerative dynamics of the flame should be considered when performing a safety management analysis.

In light of these considerations, the present study had the following objective: to experimentally investigate the influences of flame acceleration due to the flame instabilities of the blast wave generated by unconfined hydrogen/air deflagrations. We focused on the starting point of the flame acceleration at the transition from the stable regime to a fully cellular flame in the unstable regime and the acceleration exponents associated with the fractal dimension.

2. Experimental setup

Fig. 1 shows the schematic diagram of the experimental apparatus for the field tests. Hydrogen/air mixtures at various equivalence ratios, $\phi = 0.71, 1.06, 1.95$ and 2.99, were injected into a plastic tent (a thin vinyl sheet of 1 m^3) and ignited by electric spark. The concentration of hydrogen was measured by a gas concentration measuring instrument (Riken Keiki Co. Ltd, FI 21). In Fig. 2, the images of an expending spherical flame during hydrogen deflagration were captured using an infrared photography (a hydrogen flame is difficult to detect by visible photography) at 2000 frames per second for the different concentrations. The blast waves during unconfined hydrogen deflagrations were simultaneously recorded using piezoelectric sensors at several distances from the ignition position: 1.770 m, 3.025 m, 6.052 m and 9.938 m.

3. Results and discussions

3.1. Onset of flame acceleration

The images of flame propagation at $\phi = 1.06$ were captured using infrared and the visible photography (Fig. 2). Although the expanding hydrogen spherical flames cannot be observed by visible photography, they can be clearly observed with infrared images. This permits the analysis of the expanding spherical hydrogen flames. The flame propagation velocities and the acceleration exponents at several gas concentrations were evaluated.

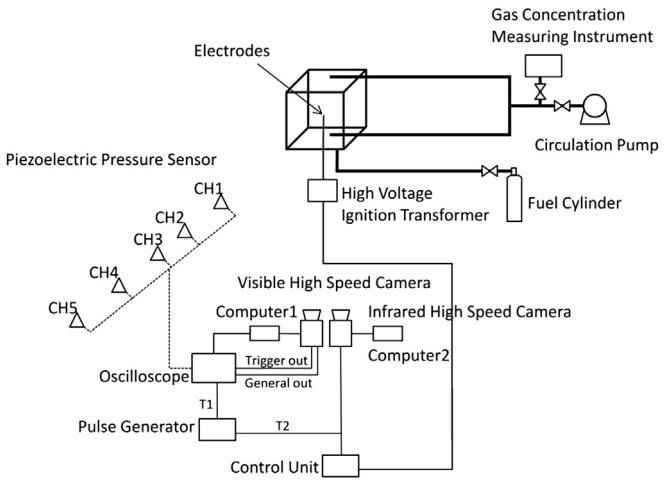

Fig. 1. Schematic diagram of experimental apparatus for the field tests.

Under conditions where the laminar flame spherically propagates without flame wrinkling, the flame radius can be written.

$$r = \varepsilon S_L t \tag{2}$$

In Fig. 3, the measured time histories of the flame radii were compared with that calculated by Eq. (2). The acceleration onset during flame propagation can be seen for various mixtures in Fig. 3. The flame acceleration onset in a lean hydrogen mixture, $\phi = 0.71$, appeared earlier than the acceleration in a rich mixture, $\phi = 2.99$. This phenomenon is because the lean flame at $\phi = 0.71$, for $Le < 1$, was strongly affected by preferential diffusion effects (diffusional-thermal instability). The flame at $\phi = 2.99$ was wrinkled and accelerated as the flame radius grew larger. This is due to hydrodynamic instability. It is known that hydrodynamic instability has a more significant effect as the flame scale increases, whereas the diffusional-thermal instability is influential even if the flame scale is small. On the other hand, the flame of a lean hydrogen mixture is continuously accelerated by diffusional-thermal instability (from an early stage) and hydrodynamic instability (from a later stage). On the other hand, the flame of a rich mixture was smoothly propagated until the flame acceleration onset owing to hydrodynamic instability.

In Fig. 4, the measured flame propagation velocity was plotted against the flame stretch rate (calculated by the flame radius). The flame stretched rate of the spherical flame propagation K is given as

$$K = \frac{1}{A}\frac{dA}{dt} = \frac{2}{r}\frac{dr}{dt} \tag{3}$$

The stretch effect of an outwardly propagating spherical flame was the greatest at the initial stage of the propagation (where K is large) and progressively decreased as the flame continues to propagate (Law, 2006, chap. 10) (K becomes smaller). As seen in Fig. 4, the measured flame propagation velocity suddenly increases for some values of α, corresponding to the points where flame acceleration onset occurs. The flame radius, r_c, at these critical points can be determined from the figure (Gu, Haq, Lawes, & Woolley, 2000; Haq, 2005). The measured value of the critical flame radius, r_c, were approximately $r_c = 0.1$ m and 0.19 m at $\phi = 0.71$ and $\phi = 2.99$, respectively. Although the values are quite smaller than that reported by Gostintsev et al. (1988), these values were similar to the experimental results reported in the previous works (Bradley et al., 2001; Dobashi et al., 2011; Nishimura et al., 2013).

3.2. Acceleration exponents and fractal dimensions

The flame radius r can be expressed as $r \approx t^{1/(3-d)}$ where t is the time from ignition and d is the fractal dimension of the flame front given by fractal theory (Gostintsev et al., 2004, 1988). Gostintsev et al. suggested that the acceleration exponents, $\alpha = 1/(3-d)$ approaches 3/2 under similar turbulization conditions. This indicates that the fractal dimension is 7/3. Such characteristic values of self-acceleration have also been reported in several studies (Aldredge & Zuo, 2001; Bradley et al., 2001; Filyand, Sivashinsky, & Frankel, 1994).

Fig. 5 is the logarithmic plot of the experimental flame radius as a function of time at $\phi = 0.71$ and $\phi = 2.99$. The plot of r–t is not exactly linear, and the value of the exponent was not constant during flame propagation. In the experiments, the value of the exponent progressively increased and did not reach $\alpha = 3/2$. Consequently, the different values of the exponent were obtained by the slope of r–t at different times during the propagation.

Fig. 6 shows the relationship between the measured acceleration exponents and the flame radius at $\phi = 0.71$ and $\phi = 2.99$. The results demonstrate that the spontaneous-acceleration ($\alpha > 1$)